Critical Initiation of Curved Unsteady Detonation in Noble-Abel and van der Waals Gas

Zifeng Weng[a], Rémy Mével[b]
[a] School of Vehicle and Mobility, Tsinghua University, Beijing, 100084, China
[b] School of Aeronautics and Astronautics, Zhejiang University, Hangzhou, 310027, China

1 Motivations

Direct detonation initiation (DDI) refers to the initiation of a detonation via intense energy release by a point energy source. In practice, the point energy source can be a piece of solid explosive, an exploding wire, or an electric spark [1]. A blast wave is formed after the energy release. When the energy of the point source is largely above the critical value (E_c), the detonation is established instantaneously and its velocity decays and asymptotically reaches the theoretical Chapman-Jouguet velocity (D_{CJ}) after some distance. In case of critical detonation initiation, i.e., the energy of the point source is close to the critical value, the velocity of the blast wave decreases to below D_{CJ}, stabilizes within the so-called quasi-steady period, and then increases to form an over-driven detonation, which finally relaxes to a CJ detonation. If the initiation energy is significantly below the critical value, the blast wave velocity continuously decreases and eventually becomes a simple acoustic wave [4]. There have been a number of works building theoretical models for the critical state of DDI. Among them, two important theories, i.e., the critical curvature (CC) [2], and the critical decay rate (CDR) [1] models, were fundamental. In the CC theory, He and Clavin proposed that critical initiation mainly depends on the curvature of the detonation front. By neglecting the unsteady effects, a critical radius was derived in their analysis [2]. In contrast, the CDR model assumes the unsteadiness, and the associated volumetric expansion behind the decaying leading shock, is responsible for the critical state of DDI. Overall, the CDR theory seems more accurate since the critical initiation energy obtained via the CDR model agrees better with experimental results [1, 8]. However, all these theoretical models were based on the perfect gas (PG) assumption. Recently, the authors have extended the CDR theory from perfect gas to Noble-Abel (NA) and van der Waals (vdW) gas [7]. It was shown that the finite molecular volume tends to promote detonation initiation, while the attractive intermolecular forces have the opposite effect. However, the effect of curvature was ignored. The goal of the present study was to investigate the effect of curvature on the initiation of a detonation behind an unsteady, decaying shock wave propagating in a high-pressure gas.

2 Methodology

An asymptotic analysis was performed for the reactive Euler equations. The detonation propagation was assumed to be axis-symmetric which reduces the problem to one-dimension. Following the methodology of Eckett et al. [1] and Weng et al. [7], the derivative of the temperature (T) along the path of a

Correspondence to: mevel@zju.edu.cn

Lagrangian particle was obtained from the reactive Euler equations as

$$\underbrace{\eta\frac{\mathrm{D}T}{\mathrm{D}t}}_{\text{Total}} = \underbrace{-\frac{\left(1-\gamma M^2\right)}{\gamma c_v}\sum_k \Omega_k\left(\frac{\partial e}{\partial y_k}\right)_{T,\rho,y_{i\neq k}} - \frac{\gamma-1}{\gamma}\left(\frac{\partial T}{\partial P}\right)_{\rho,\mathbf{Y}}\sum_k \Omega_k\left(\frac{\partial P}{\partial y_k}\right)_{T,\rho,y_{i\neq k}}}_{\text{Heat release}}$$
$$+\underbrace{\rho\frac{\gamma-1}{\gamma}\left(\frac{\partial T}{\partial P}\right)_{\rho,\mathbf{Y}} w^2\frac{j}{R_S-x}\left(U_S-w\right)}_{\text{Curvature}} + \underbrace{\rho\frac{\gamma-1}{\gamma}\left(\frac{\partial T}{\partial P}\right)_{\rho,\mathbf{Y}}\left(w\frac{\mathrm{d}U_S}{\mathrm{d}t} - w\frac{\partial w}{\partial t} + \frac{1}{\rho}\frac{\partial P}{\partial t}\right)}_{\text{Unsteadiness}}. \tag{1}$$

where $\eta = 1 - M^2$ is the sonic parameter; M is the Mach number; $\mathrm{D}/\mathrm{D}t$ is the material derivative; t is the time; γ is the heat capacity ratio; c_v is the heat capacity at constant volume; e is the internal energy; Ω_k and y_k are the production rate and mass fraction of species k, respectively; P is pressure; ρ is density; w is the flow speed in the shock-attached frame of reference; R_s indicates the shock location; x is the spatial coordinate in the frame of reference attached to the shock wave; U_S is the shock speed; j is the geometrical factor, i.e., j=0, 1, 2 for planar, cylindrical and spherical geometry. For the ease of theoretical analysis, a one-step irreversible reaction, i.e., $\mathcal{R} \rightarrow \mathcal{P}$ was assumed. The rate of progress is described by

$$\Omega_{\mathcal{P}} = F\phi_{\mathcal{R}}\left(1-y_{\mathcal{P}}\right)\exp\left(\frac{-E_a}{R_u T}\right). \tag{2}$$

where F is the pre-exponential factor; E_a is the activation energy; and R_u is the universal gas constant; $\phi_{\mathcal{R}}$ is the fugacity coefficient. To close the governing equations, the NA and vdW equations of state (EoS) were employed

$$P = \begin{cases} \dfrac{\tilde{R}T}{v-b}, \text{ NA EoS;} \\ \dfrac{\tilde{R}T}{v-b} - \dfrac{a}{v^2}, \text{ vdW EoS;} \end{cases} \tag{3}$$

where $\tilde{R}$ is R_u divided by the mean molar mass (W) of the mixture, $v = 1/\rho$ is the specific volume. The finite molecular volume was described by the covolume parameter b, while the intermolecular attraction parameter was described by a.

In the asymptotic analysis, variables were expanded based on large reduced activation energy, i.e., $\theta = E_a/R_u T_s >> 1$. The temperature was approximated to the first-order (Eq. 4), while other variables were approximated with their values at the postshock state. $\hat{T}_1$ is the non-dimensional temperature; the subscripts s designates the postshock conditions. The details were presented in [1, 7]. In addition, it was also assumed that the front radius was much larger than the reaction zone thickness. With these assumptions, Eq. 1 was reduced to an ordinary differential equation of $\hat{T}_1$ (Eq. 5).

$$\frac{T}{T_s} = 1 + \frac{1}{\theta}\hat{T}_1 + O\left(\frac{1}{\theta^2}\right). \tag{4}$$

$$\begin{aligned} &\frac{\mathrm{D}\hat{T}_1}{\mathrm{D}\varsigma} = e^{\hat{T}_1} + \frac{jU_S}{R_S}\alpha_{\text{cur}} + \frac{1}{U_S}\frac{\mathrm{d}U_S}{\mathrm{d}t}\alpha_{\text{uns}}. \\ &\text{where } \varsigma = \frac{t-t_i}{\tau_i}, \quad \alpha_{\text{cur}} = \frac{\gamma_s-1}{\gamma_s}\frac{\rho_s}{T_s}\frac{\theta\tau}{1-M_s^2}\left(\frac{\partial T}{\partial P}\right)_{\rho,\mathbf{Y}} w_s^2\left(1-\frac{w_s}{U_S}\right), \\ &\alpha_{\text{uns}} = \frac{\gamma_s-1}{\gamma_s}\frac{\rho_s}{T_s}\frac{\theta\tau}{1-M_s^2}\left(\frac{\partial T}{\partial P}\right)_{\rho,\mathbf{Y}}\left[w_s U_S\left(1-\frac{\partial w_s}{\partial U_S}\right) + \frac{U_S}{\rho_s}\frac{\partial P_s}{\partial U_S}\right]. \end{aligned} \tag{5}$$

ς is the non-dimensional time; t_i refers to the time at which the fluid particle is crossing the shock; τ_i is the asymptotic ignition delay time; α_{cur} and α_{uns} respectively characterize the impact of curvature and unsteadiness on the state of the Lagrangian particle.

$$\tau = \frac{1}{F\phi_{\mathcal{R}}\theta}\frac{1-M_s^2}{1-\gamma_s M_s^2}\frac{\gamma_s c_v T_s}{Q}e^{\theta}, \tag{6}$$

By solving Eq. 5, the critical condition for DDI is given as the relation between the critical decay time ($t_{d,c}$) and the divergence time (t_κ), as shown in Eq. 7. The decay time characterizes the rate of detonation speed variation, while the divergence time measures the rate of detonation front area variation. Similar to [7], the critical condition was studied at the CJ speed in the following context.

$$\begin{aligned} &\frac{\alpha_{uns,i}}{t_{d,c}} - \frac{\alpha_{cur,i}}{t_\kappa} = 1. \\ &\text{where } t_\kappa = \frac{A(t)}{dA(t)/\mathrm{d}t} = \frac{R_S}{jU_S}, \quad t_d = -\frac{U_S}{\mathrm{d}U_S/\mathrm{d}t} \end{aligned} \tag{7}$$

In order to relate the critical condition with the dynamics of blast waves, two blast wave models were considered, i.e., the Taylor-Sedov (TS) model [5, 6] and Korobeinikov's (Ko) model [3]. The Ko model accounts for the contribution of the chemical heat release of the mixture to the wave propagation, whereas the TS model ignores it. These blast wave models describe the evolution of the location and speed of the blast wave front with time for a given energy of a point energy source (E_s) and given properties of the reactive mixture. Although these models were developed for PG, they are expected to provide a physically reasonable approximation of the relationship between the decay and the divergence times for NA and vdW gas. The decay time - divergence time relations as the wave propagates at CJ speed are respectively presented in Eq. 8 and 9 for TS and Ko models. The overbar denotes the non-dimensional parameters as detailed in [7]. γ° refers to the heat capacity ratio for PG.

$$\bar{t}_d = \frac{2j}{j+1}\bar{t}_\kappa. \tag{8}$$

$$\begin{aligned} &\bar{t}_d = \frac{2j\bar{t}_\kappa}{j+1}\left(1+\frac{j+2}{j+1}\frac{C_j\bar{Q}}{\bar{U}_{\mathrm{CJ}}^2}\right)\exp\left[-\frac{C_j\bar{Q}}{(j+1)\,\bar{U}_{\mathrm{CJ}}^2}\right], \\ &\text{where } C_{j=2} = 4.1263(\gamma^\circ-1)^{1.2530+0.14936\log_{10}(\gamma^\circ-1)}. \end{aligned} \tag{9}$$

3 Results

Figure 1 presents the critical decay time - divergence time relations calculated with PG, NA and vdW EoS. For all the cases considered, the critical decay time increases with the divergence time. When the divergence time is small, corresponding to small radius of the wave front and the early stage of blast wave propagation, the critical decay time is sensitive to the divergence time. Larger curvature results in smaller divergence time and therefore leads to smaller critical decay time and easier ignition. However, as the wave propagates outwardly, the curvature effect attenuates and thus the critical decay time asymptotically approaches the one for unsteady planar detonation. Compared with the results for PG EoS, the range of divergence time in which the critical decay time is sensitive to curvature is reduced by the finite molecular volume effect, regardless of wether the attraction parameter is zero or equal to the covolume parameter. When the attraction parameter is much larger than the covolume, i.e., $\bar{a} = 5\bar{b}$, the effect of intermolecular attraction force increases the range of divergence time in which the curvature effect is important. The real gas (RG) effects on the critical decay time - divergence time relations are

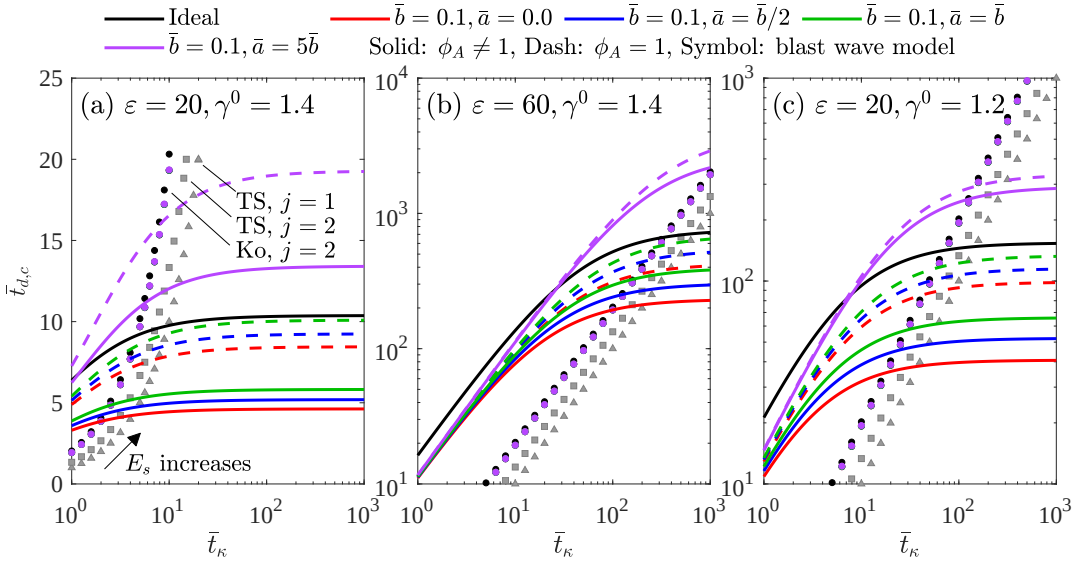

Figure 1: Critical decay time - divergence time relations for unsteady curved detonation calculated using PG, NA and vdW EoS (line) as well as blast wave models (symbol). $\bar{Q} = 30$.

affected by the properties of the mixture, i.e., ε and γ°. Figures 1(a) and 1(b) evaluate the effect of ε, while Fig. 1(a) and 1(c) assess the role of γ°. Larger ε or smaller γ° enhance the finite molecular volume and intermolecular attraction force effects on the effective range of divergence time. In addition, the critical decay time - divergence time relations for RG tend to converge at small divergence time and to diverge at large divergence time.

The decay time - divergence time relations of blast wave at CJ speed are also plotted in Fig. 1 for different wave geometries and initiation energies. Each initiation energy corresponds to a pair of critical decay time and divergence time and is shown as one point in Fig. 1. The initiation energy increases from bottom left to top right. The intersection between line and symbol corresponds to the critical initiation energy for each case. Figure 1 reveals that the finite molecular effect tends to reduce the critical initiation energy while the intermolecular interaction effect increases the critical initiation energy. The RG effect from reaction kinetic law also contributes to a lower critical initiation energy. In Fig 1(b) and Fig 1(c), the intersection is mostly located where the curvature effect is negligible, even though the curvature affects the critical decay time in a large range of the divergence time. On the contrary, the intersection in Fig 1(a) occurs at the divergence time at which curvature is still affecting the critical decay time. When considering the spherical wave and the chemical heat release in the blast wave, i.e., Ko model, the curvature affects the critical decay time to a larger extent at the critical state. In [1], the curvature effect has been neglected based on numerical simulations and order of magnitude analysis. Figure 1 implies that this assumption might not be very accurate for mixtures with large γ° and small ε and a blast wave trajectory following the Ko model. Overall, the impact of the curvature term can be taken as second-order.

To better illustrate the RG effects on the $t_{d,c}$-t_κ relation, the ratio of $t_{d,c}$ calculated with PG and RG models is presented in Fig. 2. The effect of finite molecular volume reduces $t_{d,c}$ in the whole divergence-time range compared to the results for PG, even when the covolume equals to the attraction parameter. When the attraction parameter is much larger, e.g., $\bar{a} = 5\bar{b}$, the $t_{d,c}$ ratio is larger than 1 at large divergence time, but is still smaller than 1 at small divergence time. This is because at large divergence time, the intermolecular attraction force results in larger critical decay time ratio as discussed for unsteady planar detonation [7], but the curvature term becomes more important in Eq. 7 at low divergence time. Fig-

ures 2(a) and 2(b) illustrate the RG effect from mass action law. Excluding this effect results in higher critical decay time ratio compared to the results obtained with the complete RG model. It indicates that neglecting the RG effect on kinetics lowers RG effect when the finite molecular volume effect dominates, and strengthens RG effect when the intermolecular attraction effect dominates. Figures 2(b) and 2(c) present the effect of ε while Fig. 2(b) and 2(d) demonstrate the effect of γ°. The observations are similar to that for unsteady planar detonation. Increasing ε or decreasing γ° enhance the effect of finite molecular volume and the effect of intermolecular attraction on the critical decay time. They result in smaller critical decay time ratio when the covolume effect dominates while a larger critical decay time ratio is obtained when the intermolecular attraction effect dominates.

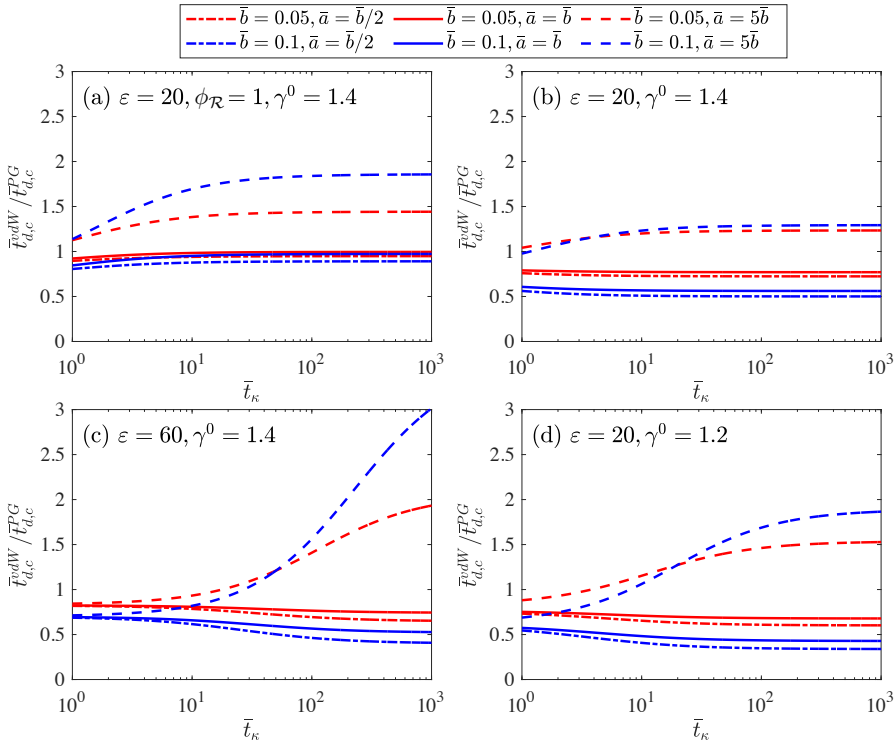

Figure 2: Impacts of the finite molecular volume and the intermolecular attraction effect on the $t_{d,c}$-t_{κ} relation for unsteady curved detonation calculated using vdW EoS. $\bar{Q}=30$. (a) is plotted by setting $\phi_{\mathcal{R}}=1$ to neglect the RG effects on mass action law.

Additional analysis focus on the chemical reaction model. A quasi-unsteady simulation was performed with detailed chemistry following [1, 7] to validate the theoretical results based on simplified reaction model. The critical state was determined when the thermicity peak reduces to 1% of its value in ZND model ($\dot{\sigma}_{\max}$). The 0.1% and 10% values were also used to represent the upper and lower boundaries of the critical state. Fig. 3 presents the comparison between quasi-unsteady simulation and asymptotic solutions for the $t_{d,c}$-t_{κ} relation. The results were calculated using both NA and vdW EoS for stoichiometric H_2-air and C_2H_4-air mixtures. We fixed the value of $\bar{b}$ at 0.1 and the temperature at 300 K. The value of the parameter $\bar{a}$ can be determined by the EoS and mixture composition. It falls in the range 0.071-1.278 for H_2-air mixture and within 0.160-0.198 for C_2H_4-air mixture. The quasi-unsteady results are qualitatively similar to the asymptotic solutions. The difference between the two models increases at large divergence time, as the curvature effect becomes negligible. For example, for the H_2-air mixture, the difference is relatively large at large divergence time, but decreases as the divergence time reduces. For the C_2H_4-air mixture, since the critical decay times of the two models match well for unsteady planar detonation, the results of the two models for unsteady curved detonation are close in the whole

range of t_κ. It should be noted that the results calculated with NA are close to the results obtained using vdW EoS. For the mixtures and conditions we selected, since the attraction parameter is not much larger than the covolume, the intermolecular attraction effect does not have significant impact on the results.

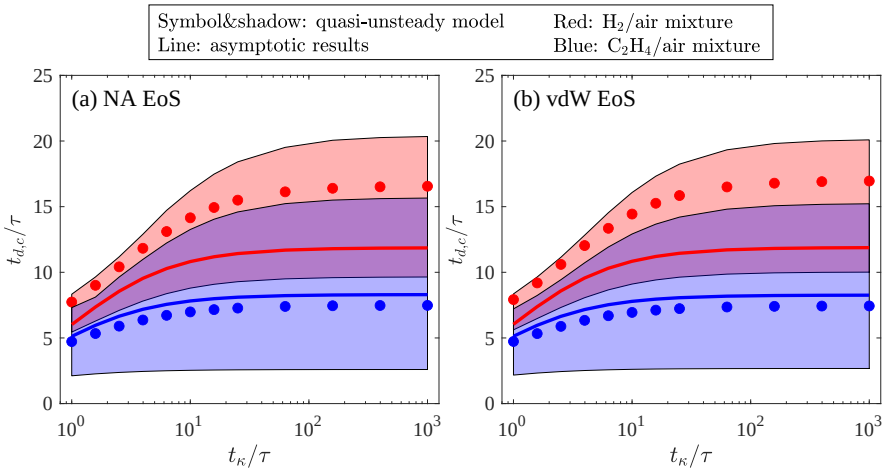

Figure 3: Comparison of quasi-unsteady model results (symbol and shadow) and asymptotic solutions (line) calculated with NA and vdW EoS. The $t_{d,c}$ was normalized with the induction time of ZND model. Solid circle: 1% of $\dot{\sigma}_{\max}$; upper and lower boundary of shadow: 10% and 0.1% $\dot{\sigma}_{\max}^{\mathrm{ZND}}$, respectively.

In summary, the asymptotic analysis demonstrated that the curvature term only has secondary impact on the critical state of direct detonation initiation. It is because, when the critical condition is satisfied, the radius of blast wave is relatively large, and accordingly, the curvature effect is limited. The findings of asymptotic analysis are also supported by quasi-unsteady simulation using detailed reaction models. In the future, it would be relevant to compare the predictions of our model to experimental data obtained at high-pressure conditions, if such measurements become available in the literature.

References

[1] Eckett CA, Quirk JJ, Shepherd JE. (2000). The role of unsteadiness in direct initiation of gaseous detonations. J. Fluid Mech., 421:147–183.

[2] He L, Clavin P. (1994). On the direct initiation of gaseous detonations by an energy source. J. Fluid Mech., 277:227–248.

[3] Korobeinikov V. (1968). Point explosion in a detonating gas. Soviet Doklady Physics, 12:1003–1005.

[4] Lee JHS. (2008). The Detonation Phenomenon. Cambridge University Press.

[5] Sedov L. (1960). Similarity and dimensional methods in mechanics. CRC Press.

[6] Taylor G. (1950). The formation of a blast wave by a very intense explosion I. theoretical discussion. Proc. R. Soc. Lond. A, 201:159–174.

[7] Weng Z, Mével R, Law C. (2023). On the critical initiation of planar detonation in Noble-Abel and van der Waals gas. Combust. Flame, 255:#112890.

[8] Weng Z, Mével R, Huang Z, Cai F, Xu J. (2021). Direct detonation initiation: A comparison between the critical curvature and critical decay rate models. Phys. Fluids, 33(9):#096110.